ELSEVIER

Sensors and Actuators A 46–47 (1995) 576–579

SENSORS AND ACTUATORS A PHYSICAL

Micro-windmill for optical scanning and flow measurement

Mark Ross, Kristofer S.J. Pister

Electrical Engineering Department, University of California, Los Angeles, CA 90024, USA

Abstract

This paper reports on the development of a micro-windmill. The device consists of a 0.6 mm diameter rotor with four spokes connecting a 10 μm wide outer ring with a 10 μm wide inner ring. A hinged polysilicon plate along each spoke is water-assembled or manually assembled to stand 100 μm high. Rotation of the windmill has been observed in an air stream with pressure of less then 40 N/m^2. However, the windmill would not spin under the same conditions when the air stream pressure was 26 N/m^2. The micro-windmill has been successfully used as an optical scanner, with angular repeatability of 5° and angular variation of 2° perpendicular to the scan direction.

Keywords: Micro-windmill; Optical scanning

1. Introduction

Microelectromechanical structures have quickly evolved from a field consisting of cantilevers and membranes to a point where the integration of submillimeter electric and mechanical parts into simple systems is becoming feasible, and for some simple systems, nearly cookbook. The field is rapidly changing because so many basic macroscale elements are being sequentially demonstrated on a microscale.

Micromachined pin joints for rotary motion were first developed in 1987 by Fan et al. [1]. Soon after, several researchers produced operating electrostatic micromotors [2–4].

The introduction of microhinges [5] into the field of microelectronics processing has provided a new means for implementing three-dimensional structures by means of surface micromaching. Self-assembling techniques for three-dimensional structures [6] allow for structural stability by locking the microhinges into allowed positions. By adding hinged plates to a rotating microwheel, a micro-windmill is achieved.

The micro-windmill has applications ranging from a flow measurement device to an optical scanner. The optical scanner consists of a rotating reflector standing perpendicular to the plane of the chip onto which light may be shone. By rotating the reflector the incident light may be reflected. Macroscale optical scanners are commonly used in both a constant velocity mode or a position addressable mode.

2. Design

The windmill system consists of a pinned rotor [1] with four hinged plates which pop up out of their plane of fabrication (Figs. 1 and 2). Scissor hinges [6] were used, rather than single pin hinges, to allow for separation of the hinge from the substrate while not requiring a third polysilicon layer for constraint. The system is designed for fabrication in a two polysilicon process, such as the MUMPS process of MCNC.

The wheel consists of a pinned inner ring with inner radius 10 μm and outer radius 20 μm connected to an outer ring with inner radius 310 μm and outer

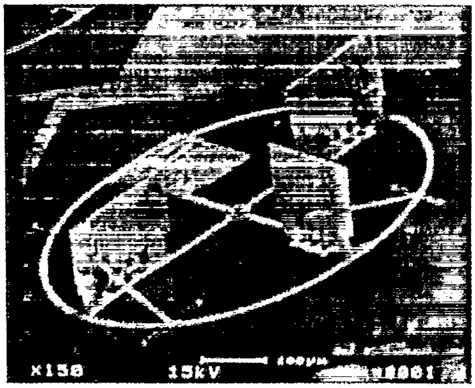

Fig. 1. SEM of 0.6 mm diameter micro-windmill with three blades erected and one blade in original fabrication position. Spring locks keep the three erected blades erect during rotation of the device. The dark and light colors in the blades shown on the SEM are due to the two layers of polysilicon composing the blade, each having its own conductivity.

0924-4247/95/$09.50

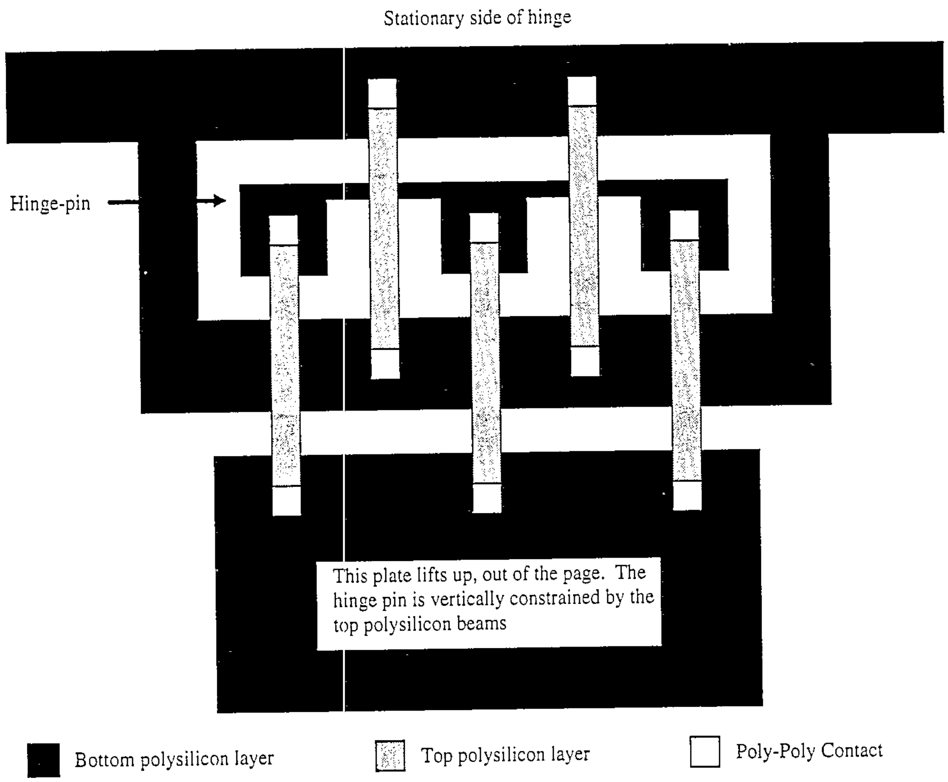

Fig. 2. Physical layout of the scissor hinge structure. This diagram illustrates the relations between the two polysilicon layers.

radius 320 μm by spokes 10 μm wide. This is all fabricated with polysilicon 2 μm thick. The pin constraining this wheel contacts the substrate with a 14 μm diameter circle and overhangs the inner wheel to a radius of 15 μm.

Scissor hinges connect the pop-up fins to the spokes of the wheel. These scissor hinges are two completely separate pieces of polysilicon which are looped together to keep from separating during rotation. The scissor hinges consist of a hinge pin 2.5 μm wide, made of the first polysilicon layer, contacting three beams of the top polysilicon layer connecting to the pop-up fin consisting primarily of the first polysilicon layer. The hinge pin is constrained from above by two bars of the top polysilicon which connect to the side constraints of the first polysilicon. The pin is constrained from below by the silicon nitride substrate.

Each pop-up fin consists of a 200 $\mu m \times 100$ μm plate connected to a spoke of the wheel by a scissor hinge. The plate is comprised of a combination of both polysilicon layers, individually and together.

The spokes were extended to provide supports for the fins, collinear with the hinges, where tabs from the plates could fit in slots to ensure proper positioning upon erection of the fins. Additionally, torsional spring locks were included to provide additional support and constraint to the erected plates. The spring locks, when properly engaged, constrain a point in the fin to 1.5 μm of motion in either direction at a height 50 μm from the substrate. This locked position is the one stable position for the erected fins. The torsional spring locks consist of a spring loop extending 50 μm in either direction, rejoining into a beam, nominally 8 μm wide and 240 μm long. At the point where this beam should intersect the standing plate, the beam narrows to a width of 3 μm for 3 μm. This narrowed section fits into a V-shaped slot in the rotated fin, locking it in place (Figs. 3 and 4). These dimensions were chosen

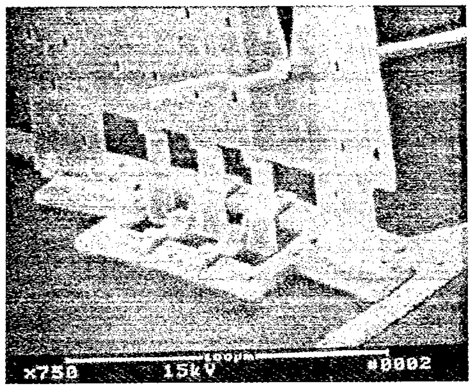

Fig. 3. Close-up of scissor-hinged windmill fin locked in standing position by torsional spring lock. Some of the fins self-assembled in the rinse tank during the sacrificial etch while others were manually assembled with probe tips. The through-holes in the standing plate reduce release time by providing more points for HF access under the plate. The pits in the standing plate are 'dimples' which suspend most of the plate a dimple-height above the substrate after the oxide layer has been removed in order to reduce the contact area between the plate and the substrate. Notice the tabs on either side of the hinge are not falling into the slots behind them. Resultantly, the beam with the slot is bowed.

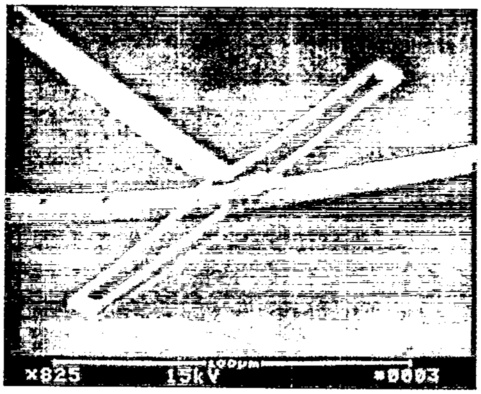

Fig. 4. Close-up flexural spring attached to outer ring. The flexures are 2 μm×1.5 μm, and extend 50 μm in either direction. Dimples along outer ring to reduce contact area with substrate are visible.

larger than the 2 μm minimum dimension for the MUMPS2 process to ensure structural integrity.

All of the polysilicon is dimpled for reduced sticking to the substrate after the HF release etch. To facilitate HF access to the oxide under the large plates, small holes are designed into the polysilicon in all areas in which the polysilicon extends more than 10 μm in all directions.

3. Experimental

A stream of nitrogen gas was blown at the micro-windmill to demonstrate its motion. The micro-windmill spun when blown with nitrogen through the pipette with 40 Pa. A pressure of 26 Pa, however, was not sufficient to turn the windmill. The windmill was seen to spin at a rate greater than 100 rpm. Once the windmill began spinning, it would remain spinning while the nitrogen was blowing it.

Two windmill structures were spun with a probe tip to determine how erect the fins remain during spinning. This was done manually so that there will be minimum turbulent air flow around the hinged structures which causes them to sway. The two structures used differ only in that one has a torsional lock holding the hinged plate in its upright position. A laser beam, parallel to the plane of the chip, with a spot size greater than 1 mm diameter was shone on to the windmill structure in a manner that would allow the beam to be reflected off of the faces of two of the windmill blades on to a scale perpendicular to the incident beam 14 cm from the windmill and on to another scale parallel to the incident beam 20 cm from the windmill (Fig. 5). The windmill was manually rotated a few degrees at a time and measurements of the reflected beam position were taken. The graph in Fig. 6 compares the visually measured angle of rotation of the mirror with the angle calculated from the position of the reflected beam.

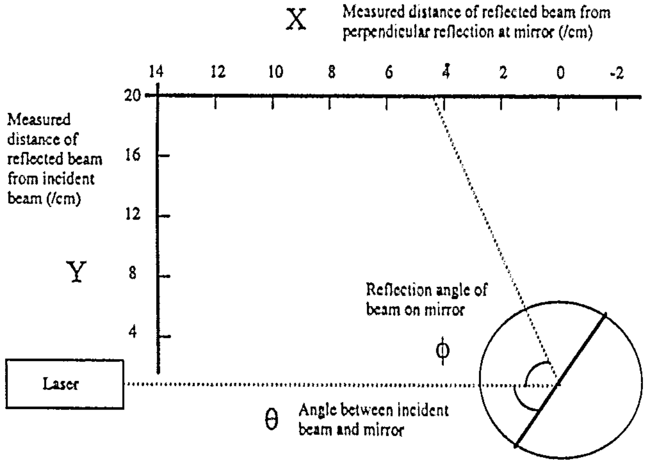

Fig. 5. Schematic of optical setup for measuring position of reflected beam as a function of angle of the mirror. Angle of the mirror to the laser beam was measured visually, through a microscope and calculated from the position of the reflected beam on the two scales.

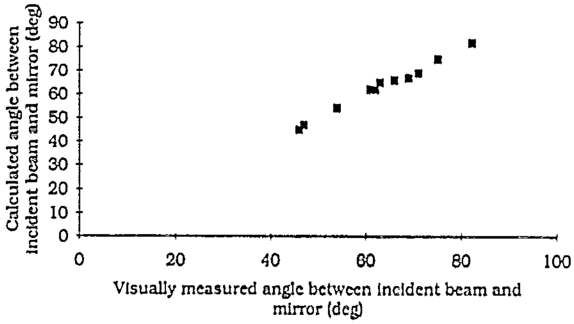

Fig. 6. Comparison of angle of the reflected beam with visually measured angle of windmill.

During the above measurements, the reflected beam moved 5 mm or less perpendicular to the direction of scanning. This motion of the beam corresponds to a rotation of the mirrors of under 2°.

The windmill structures without the torsional spring locks to support the plates in an upright position could not be rotated more than 5° without the plates falling back down to the substrate.

4. Discussion

For the windmill with torsional spring locks, the data show that the reflected beam angle is repeatable 5°. Also, for this structure, the blades remained locked in their upright position to within 2° based on the measurement that the reflected beam only varied by about 5 mm in the direction perpendicular to the rotation at a distance of 20 cm from the windmill. The spring locks in the present windmill have 3 μm of travel. For the 2 μm process used to fabricate this device, that parameter can be lowered to 2 μm. That would reduce the sway from an allowed 1.7° to either side of vertical to 1.1° to either side of vertical, corresponding to a perpendicular beam variation of only 7 mm at a distance of 20 cm. Additionally, the torsional spring lock can be located higher on the windmill (from 50 μm from the substrate, where it is presently, to 75 μm from the substrate), constraining it to motion of only 0.76° in either direction from the vertical, which corresponds to a deflection of 5 mm at a distance of 20 cm.

The blades on the windmill structure without torsional locks flapped about with angles often greater than 30° perpendicular to the scan direction, making it unsuitable for most applications.

The 100 μm×200 μm plates are large enough to cause little diffraction of the reflected beam. Only one reflected beam was observed despite the two windmill blades reflecting the laser light.

5. Potential applications

The lock-supported reflector structure may be used to replace much larger polygon mirrors for beam-scanning applications. Motorization of this reflector structure could have application in such systems as scanners for laser printers, fax machines, and supermarket scanners. A representative commercial motorized polygon mirror (manufactured by Japan Electronics) has a ten-sided first surface mirror which spins at a constant rate of 26 000 rpm and sells for a few hundreds of dollars. A spinning reflector system need only spin at a rate of a few tens of Hz to be useful for a variety of applications. Gabriel et al. [7] have observed a planar rotator, driven by air blown through a pipette, rotating at 600 000 rpm.

If the reflector structure is electrostatically motorized [8], then the reflecting plates could be initially fabricated laying radially outwards from an inscribed polygon of chords of the outer ring. The outer ring would also be removed except near the vertices of the polygon for action of the motor. A system such as this could have application in the low-end galvanometric scanner market, where products with maximum speeds as low as 50° per second with 0.3% linearity and 0.01% repeatability are still sold [9]. A typical MEMS micromotor speed ranges from 200 to 2000 rpm [8]. The described micromachine meets the speed requirements for entering this market. The cost of such galvanometers with mirrors ranges from several hundred to thousands of dollars each.

Conclusions

A micro-windmill has been developed. The micro-windmill consists of a 0.6 mm diameter rotor with four spokes connecting a 10 μm wide outer ring with a 10 μm wide inner ring. Along each spoke is a hinged polysilicon plate which erects to 100 μm high. Rotation of the device has been observed.

The micro-windmill has been successfully used as an optical scanner, with angular repeatability of 5° and angular variation of 2° perpendicular to the scan direction.

Acknowledgements

The authors thank P. Nelson for her assistance with the SEM and acknowledge ONR for their support.

References

[1] L.-S. Fan, Y.-C. Tai and R.S. Muller, Pin joints, gears, springs, cranks, and other novel micromechanical structures, *4th Int. Conf. on Solid-State Sensors and Actuators (Transducers '87), Tokyo, Japan, 2–5 June, 1987*, pp. 849–852.

[2] L.-S. Fan, Y.-C. Tai and R.S. Muller, IC-processed electrostatic micromotors, *Int. Electron Devices Meet., San Francisco, CA, USA, 11–14 Dec., 1988*, pp. 666–669.

[3] M. Mehregany, S.F. Bart, L.S. Tarrow, J.H. Lang, S.D. Senturia and M.F. Schlecht, A study of three microfabricated variable-capacitance motors, *Sensors and Actuators, A21–A23* (1990) 173–179.

[4] W. Trimmer and R. Jebens, Harmonic electrostatic actuators, *Sensors and Actuators, 20* (1989) 17–24.

[5] K. Pister, M. Judy, S. Burgett and R. Fearing, Microfabricated hinges, *Sensors and Actuators A, 33* (1992) 249–256.

[6] S.R. Burgett, K.S.J. Pister and R.S. Fearing, Three-dimensional structures made with microfabricated hinges, *Micromechanics, ASME Winter Annu. Meet., Anaheim, CA, USA, Nov. 1992.*

[7] K.J. Gabriel, F. Behi, R. Mahadevan and M. Mehregany, In situ friction and wear measurements in integrated polysilicon mechanisms, *Sensors and Actuators, A21–A23* (1990) 184–188.

[8] L.S. Tavrow, S.F. Bart and J.H. Lang, Operational characteristics of microfabricated electric motors, *6th Int. Conf. Solid State Sensors and Actuators (Transducers '91), San Francisco, CA, USA, 24–28 June, 1991*, pp. 877–881.

[9] *Optical Scanning Systems*, Catalog GSI700160, General Scanning, Inc., Watertown, MA, USA.